OBSTETRICS

Evidence that fetal death is associated with placental aging

Kaushik Maiti, PhD; Zakia Sultana, MPharm; Robert J. Aitken, PhD, ScD; Jonathan Morris, PhD, MBBS; Felicity Park, MBBS; Bronwyn Andrew, MBBS; Simon C. Riley, PhD; Roger Smith, PhD, MBBS

BACKGROUND: The risk of unexplained fetal death or stillbirth increases late in pregnancy, suggesting that placental aging is an etiological factor. Aging is associated with oxidative damage to DNA, RNA, and lipids. We hypothesized that placentas at >41 completed weeks of gestation (late-term) would show changes consistent with aging that would also be present in placentas associated with stillbirths.

OBJECTIVE: We sought to determine whether placentas from late-term pregnancies and unexplained stillbirth show oxidative damage and other biochemical signs of aging. We also aimed to develop an in vitro term placental explant culture model to test the aging pathways.

STUDY DESIGN: We collected placentas from women at 37-39 weeks' gestation (early-term and term), late-term, and with unexplained stillbirth. We used immunohistochemistry to compare the 3 groups for: DNA/RNA oxidation (8-hydroxy-deoxyguanosine), lysosomal distribution (lysosome-associated membrane protein 2), lipid oxidation (4-hydroxynonenal), and autophagosome size (microtubule-associated proteins 1A/1B light chain 3B, LC3B). The expression of aldehyde oxidase 1 was measured by real-time polymerase chain reaction. Using a placental explant culture model, we tested the hypothesis that aldehyde oxidase 1 mediates oxidative damage to lipids in the placenta.

RESULTS: Placentas from late-term pregnancies show increased aldehyde oxidase 1 expression, oxidation of DNA/RNA and lipid, perinuclear location of lysosomes, and larger autophagosomes compared to placentas from women delivered at 37-39 weeks. Stillbirth-associated placentas showed similar changes in oxidation of DNA/RNA and lipid, lysosomal location, and autophagosome size to placentas from late-term. Placental explants from term deliveries cultured in serum-free medium also showed evidence of oxidation of lipid, perinuclear lysosomes, and larger autophagosomes, changes that were blocked by the G-protein-coupled estrogen receptor 1 agonist G1, while the oxidation of lipid was blocked by the aldehyde oxidase 1 inhibitor raloxifene.

CONCLUSION: Our data are consistent with a role for aldehyde oxidase 1 and G-protein-coupled estrogen receptor 1 in mediating aging of the placenta that may contribute to stillbirth. The placenta is a tractable model of aging in human tissue.

Key words: aging, aldehyde oxidase 1, autophagosome, DNA/RNA oxidation, fetal death, G-protein-coupled estrogen receptor 1, lipid oxidation, placenta, placental explant culture, raloxifene, stillbirth

Introduction

Unexplained fetal death is a common complication of pregnancy occurring in approximately 1 in 200 pregnancies in developed countries[1] and more frequently in the developing world. While no cause has been established, the rate of fetal death rises rapidly as gestation progresses >38 weeks.[2] Johnson et al[3] proposed the operational definition of aging as an increase in risk of mortality with time, which is consistent with a role for aging in the etiology of stillbirth (Figure 1).[4] Supporting this view, a histopathological study of placentas associated with cases of unexplained intrauterine death at term revealed that 91% showed thickening of the maternal spiral artery walls, 54% contained placental infarcts, 10% had calcified areas, and 13% demonstrated vascular occlusion[5]; another study reported increased atherosclerosis,[6] changes associated with aging in other organs. Supporting a link between placental aging and stillbirth, Ferrari et al[7] recently reported that telomere length is reduced in placentas associated with stillbirth. Fetal growth restriction is also associated with both stillbirth and telomere shortening.[8] We therefore sought to determine whether placentas from women who delivered >41 completed weeks (late-term) or had stillbirth had biochemical evidence of aging. As markers of aging we chose to measure 8-hydroxy-deoxyguanosine (8OHdG) (a marker of DNA oxidation) and 4-hydroxynonenal (4HNE) (a marker of lipid oxidation) as both have been described to increase in the brain with aging, and the enzyme aldehyde oxidase (AOX), which is known to generate oxidative damage in the kidney. Aging is also known to affect the effectiveness of the intracellular recycling process that involves fusion of acidic hydrolase containing lysosomes with autophagosomes; we therefore sought changes in these intracellular organelles in the late-term placentas and those associated with stillbirth.

EDITORS' CHOICE

Cite this article as: Maiti K, Sultana Z, Aitken RJ, et al. Evidence that fetal death is associated with placental aging. Am J Obstet Gynecol 2017;217:441.e1-14.

0002-9378/free

http://dx.doi.org/10.1016/j.ajog.2017.06.015

Click Supplemental Materials and Video under article title in Contents at ajog.org

Materials and Methods

Ethics, collection, and processing of tissues

This study was approved by the human research ethics committee of the Hunter New England Health Services and the University of Newcastle, Australia. Human placentas were collected after written informed consent was obtained from the patients by midwives. Placentas were collected from women at 37-39 weeks' gestation undergoing cesarean delivery for previous cesarean delivery or normal vaginal delivery, women at ≥41 weeks'

FIGURE 1
Relationship between stillbirth and number of continuing pregnancies

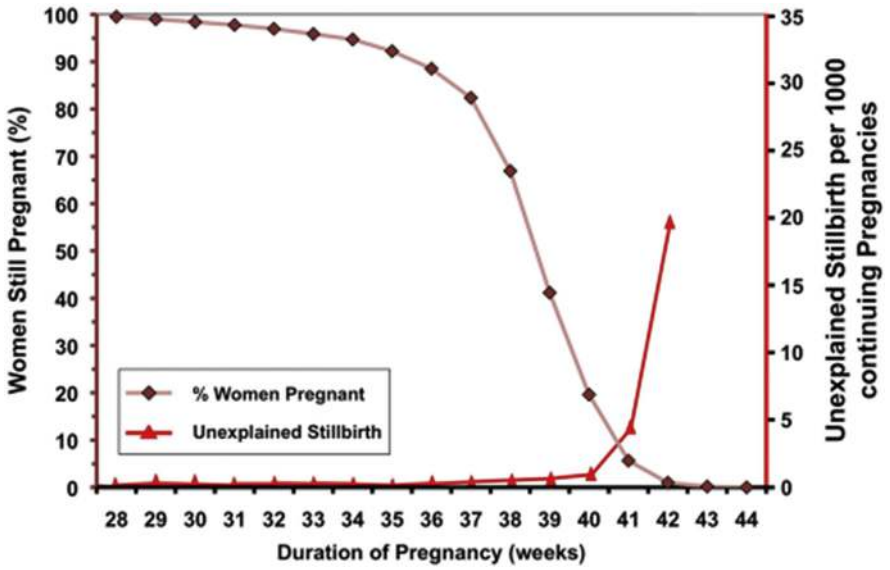

Kaplan-Meier plot of number of continuing pregnancies as function of gestational age and plot of unexplained stillbirth per 1000 continuing pregnancies; data from Omigbodun and Adewuyi[10] and Sutan et al.[2] Plot shows increase in risk of stillbirth with time consistent with operational definition of aging proposed by Johnson et al[3] and relatively small number of pregnancies at risk of stillbirth by 41 weeks because of prior delivery. Reproduced with permission.[4]

Maiti et al. Fetal death and placental aging. Am J Obstet Gynecol 2017.

gestation undergoing cesarean delivery or normal vaginal delivery, and women who had stillborn infants undergoing vaginal delivery. Placentas were collected immediately after delivery and processed without further delay. Villous tissues were sampled from multiple sites and prepared for histology and RNA extraction. For each placenta, tissues were obtained from at least 5 different regions of the placenta and 4-5 mm beneath the chorionic plate. Samples from each individual placenta were immediately frozen under liquid nitrogen and stored at −80°C until subsequent experiments. For histology experiments, tissues were fixed in 2% formaldehyde for 24 hours, stored in 50% ethanol at room temperature, and embedded in paraffin. To create a placental roll a 2-cm strip of chorioamniotic membrane was cut from the periphery of the placenta keeping a small amount of placenta attached to the membrane. The strip was rolled around forceps leaving residual placenta at the center of the cylindrical roll. The cylindrical roll was then cut perpendicular to the cylindrical axis to obtain 4-mm thick sections and fixed in formalin. Placentas from patients with infection, diabetes, preeclampsia, placenta previa, intrauterine growth restriction, or abruption were excluded.

Reagents and antibodies

Antibodies against lysosome-associated membrane protein 2 (LAMP2) and AOX1 were obtained from BD Biosciences (Sydney, Australia) and Proteintech (Rosemont, IL), respectively. Antibody against LC3B and G-protein-coupled estrogen receptor 1 (GPER1) were obtained from Novus Biologicals (Littleton, CO). Antibodies against 8OHdG and 4HNE were purchased from Abcam (Melbourne, Australia). Dulbecco modified Eagle medium (DMEM), antibiotic-antimycotic, NuPAGE (Thermo Fisher Scientific, Melbourne, Australia) precast 12-well protein gel, and prolong gold antifade mounting media with 4′,6-diamidino-2-phenylindole (DAPI), Alexa conjugated secondary antibodies were obtained from Thermo Fisher Scientific Australia Pty. The horseradish peroxide conjugated secondary antibodies were purchased from Cell Signaling Technology (Danvers, MA). Fetal bovine serum (FBS) was obtained from Bovogen Biologicals Pty Ltd (Melbourne, Australia). Protease inhibitor and phosphatase inhibitor were supplied by Roche (Sydney, Australia). Raloxifene was purchased from Sigma-Aldrich (Sydney, Australia) and G1 was supplied by Tocris-Bioscience (Bristol, United Kingdom). The BCA protein assay kit was obtained from Thermo Fisher Scientific Australia Pty. All other chemicals were purchased from either Ajax Finechem Pty Ltd (Sydney, Australia) or Sigma-Aldrich.

Placental explant culture

For in vitro experiments, human term placentas (all at 39 weeks of gestation) were obtained from women with normal singleton pregnancies without any symptoms of labor after an elective (a scheduled repeat) cesarean delivery. Placentas were collected immediately after delivery and prepared for explant culture. Villous tissues of placentas were randomly sampled from different regions of the placenta 4-5 mm beneath the chorionic plate. Tissues were washed several times with Dulbecco phosphate-buffered saline under sterile conditions to remove excess blood. Villous explants of ~2 mm^3 were dissected and placed into 100-mm culture dishes (30 pieces/dish) containing 25 mL of DMEM supplemented with 2 mmol/L L-glutamine, 1% sodium-pyruvate, and 1% penicillin/streptomycin (100×) solution with the addition of 10% (vol/vol) FBS and cultured in a cell culture chamber at 37°C temperature under 95% air (20% oxygen) and 5% carbon dioxide

FIGURE 2
DNA/RNA oxidation in late-term and stillbirth placentas

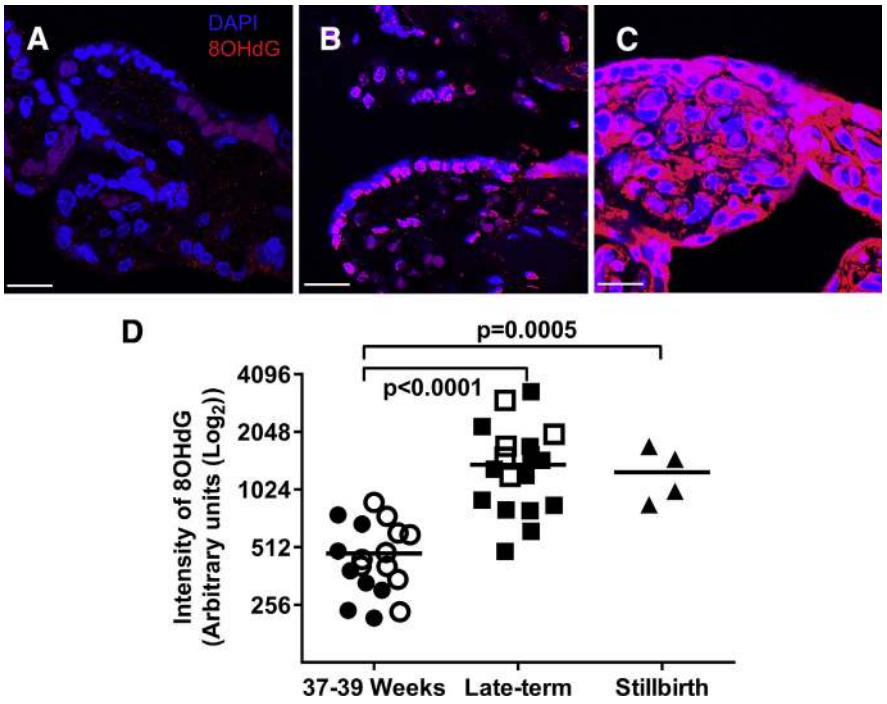

Confocal microscopy showed increased 8-hydroxy-deoxyguanosine (8OhdG) staining (red) in nuclei from **B**, late-term and **C**, stillbirth placentas compared to **A**, 37- to 39-week placentas. 4′,6-Diamidino-2-phenylindole (DAPI) (blue) staining identifies nuclei. **D**, Late-term and stillbirth placentas have increased intensity of nuclear 8OHdG staining ($P < .0001$ for late-term placentas and $P = .0005$ for stillbirth placentas, Mann-Whitney test) compared to 37- to 39-week placentas. **D**, Open and filled circles represent 37- to 39-week cesarean nonlaboring (n = 10) and vaginal delivery laboring (n = 8) placentas, respectively; open and filled squares represent late-term laboring cesarean (n = 5) and laboring vaginal delivery (n = 13) placentas, respectively; and filled triangles represent third-trimester laboring vaginal delivery unexplained stillbirth placentas (n = 4). Each point in graph represents average intensity of 8OHdG of 60 nuclei in 6 images per placenta photographed at ×100 magnification and 1.4 optical resolution. Scale bar = 20 μm. Microscopy also indicates increased staining in cytosol of late-term and stillbirth placentas representing oxidized RNA (8-hydroxyguanosine) that is also detected by antibody.

Maiti et al. Fetal death and placental aging. Am J Obstet Gynecol 2017.

for 24 hours. At day 2, villous explants were transferred to fresh 30-mL growth medium and incubated in a cell culture chamber for 90 minutes and washed in DMEM without FBS (referred to as "serum-free medium" or "growth factor deficient medium"). Next 6-7 pieces of villous tissue weighing approximately 400 mg were transferred to a culture dish (60 mm) containing 6 mL of serum-free medium with or without the addition of pharmacological agents, for example, raloxifene (1 nmol/L) or the GPER1 agonist G1 (1 nmol/L), for subsequent incubation for 24 hours. At the end of 24 hours some tissues were fixed in 2% formaldehyde, subjected to routine histological processing, and embedded in paraffin wax, and some tissues were immediately frozen in liquid nitrogen and stored at −80°C until subsequent experiments. For each placental explant culture, samples were also collected at time 0 hours, ie, before incubation in serum-free medium, and were formalin fixed and stored frozen at −80°C until further experiments.

Western blotting

Western blotting was performed as previously described.[9] Samples of placenta (1 g) were crushed under liquid nitrogen. Aliquots of 100 mg of placental tissues were homogenized in 1 mL of lysis buffer (phosphate-buffered saline, 1% Triton-X-100, 0.1% Brij-35, 1 X protease inhibitor, 1 X phosphatase inhibitor, pH 7.4). The protein concentration of each placental extract was measured using a BCA protein assay kit (Thermo Fisher Scientific) and 40 μg of placental extract was separated by electrophoresis in NuPAGE bis-tris precast 12-well gels for 50 minutes at a constant 200 V. Separated proteins were then transferred to nitrocellulose membrane using a Novex (Thermo Fisher Scientific) transfer system for 70 minutes and blocked overnight at 4°C with 1% bovine serum albumin (BSA) in tris-buffered saline with 0.1% tween-20 (TBST). The membranes were then incubated with primary antibody in 1% BSA in TBST for 2 hours at room temperature, then washed 3 times with TBST, followed by incubating with horseradish peroxide conjugated secondary antibodies in 1% BSA in TBST for an hour. After 3 further washes with TBST, the immunoreactive bands were developed in Luminata reagent (Merck Millipore, Billerica, MA) and detected using an Intelligent Dark Box LAS-3000 Imager (Fuji Photo Film, Tokyo, Japan).

Immunohistochemistry

Fluorescent immunohistochemistry (IHC) was performed according to previously published methods.[9] We deparaffinized and hydrated 6-μm paraffin placental sections, then heated them with tris-EDTA buffer (pH 9) in a microwave oven for antigen retrieval. The sections were blocked with 1% BSA in TBST for an hour at room temperature. The sections were incubated with primary antibodies overnight and washed 3 times with TBST, before incubation with Alexa-conjugated secondary antibodies for

FIGURE 3
Changes in lysosomal distribution in late-term and stillbirth placentas

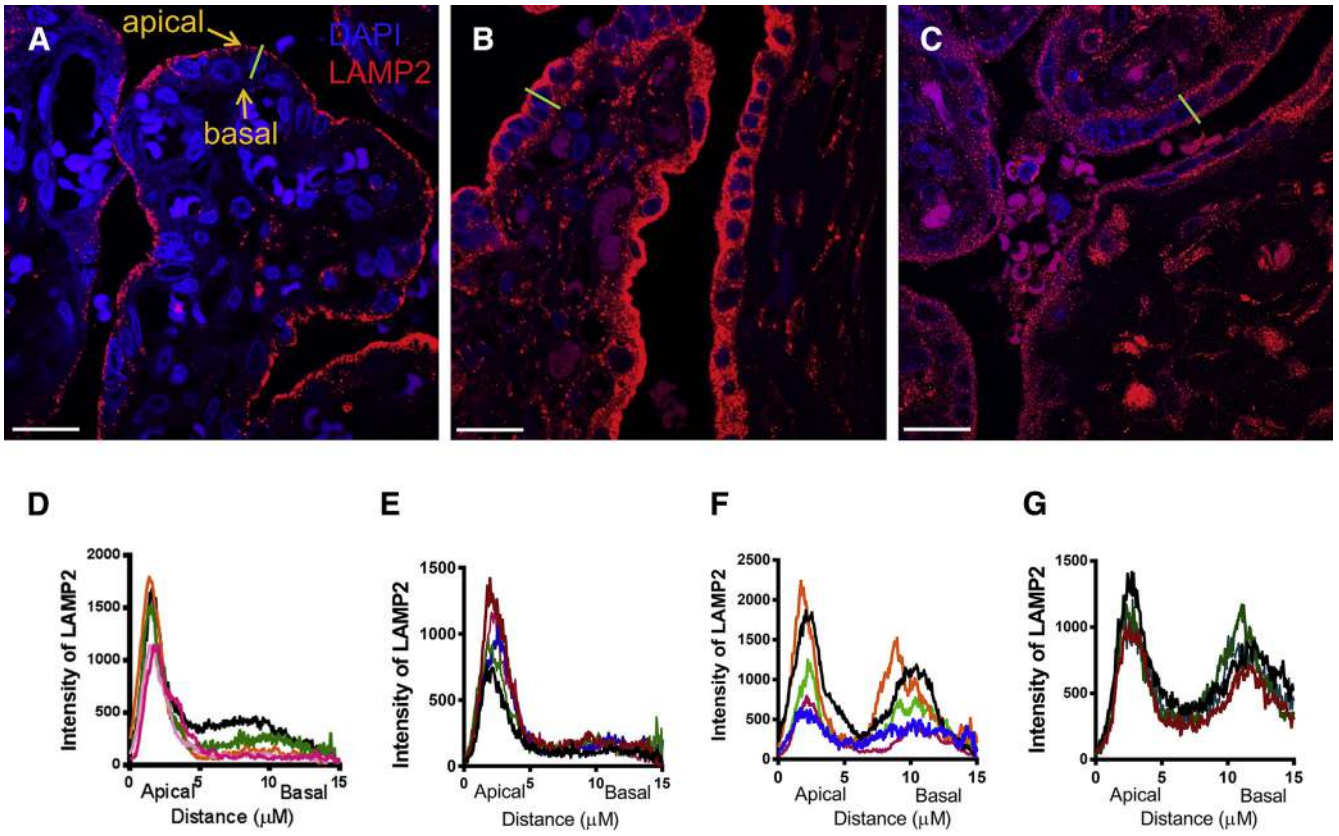

Immunohistochemistry of lysosome-associated membrane protein 2 (LAMP2) (red); lysosomal marker showed that lysosomes predominantly localize to apical surface of **A**, 37- to 39-week placentas, whereas lysosome distribution extends to perinuclear and basal surface of syncytiotrophoblast in **B**, late-term and **C**, stillbirth placentas. Intensity calculation across syncytiotrophoblast showed that distribution of LAMP2 in **F**, late-term ($n = 5$) and **G**, unexplained stillbirth ($n = 4$) placentas shifts to perinuclear and basal surface whereas lysosome distribution in **D**, 37- to 39-week cesarean ($n = 5$) and **E**, vaginal delivery ($n = 5$) placentas remained in apical region of syncytiotrophoblast. 4′,6-Diamidino-2-phenylindole (DAPI) (blue) staining identifies nuclei. **D** to **G**, Each colored line represents results on individual placenta, and shows mean intensity of LAMP2 across syncytiotrophoblast at 5 random sites per image (**A** to **C**, example represented by light green line) for 6 separate images per placenta. Images were photographed at ×100 magnification; scale bar = 20 μm.

Maiti et al. Fetal death and placental aging. Am J Obstet Gynecol 2017.

90 minutes. The sections were mounted with prolong gold antifade mounting media with DAPI. The fluorescent photographs for Figures 2 to 7 and Supplementary Figures 1 to 3 were taken on a Nikon eclipse 90i confocal microscope (Nikon Instruments Inc, Melville, NY). The fluorescent photographs for Figure 8 were taken on Nikon eclipse Ti fluorescence microscope (Nikon Instruments Inc).

RNA isolation and real-time polymerase chain reaction

Placental tissues were crushed under liquid nitrogen. Approximately 100 mg of crushed placental tissues were homogenized in 2 mL of Trizol reagent (Thermo Fisher Scientific) with an Ultra Turrax (IKA Works, Staufen im Breisgau, Germany) homogenizer. Total RNA was extracted from the Trizol-extract by Direct-zol RNA MiniPrep (Zymo Research, Irvine, CA). The RNA was treated with DNAse and purified with a RNA Clean and Concentrator-5 kit (Zymo Research). The RNA quality was checked by running the DNAse-treated sample in agarose gel with ethidium bromide in 1X Tris-acetate-EDTA buffer. The purified RNA was used to make complementary DNA using a SuperScript III first-strand synthesis system kit (Thermo Fisher Scientific), The complementary DNA was used to run real-time polymerase chain reaction (PCR) by TaqMan primers for AOX1 (assay ID: Hs00154079_m1; Thermo Fisher Scientific) and TaqMan gene expression master mix (Thermo Fisher Scientific) with an internal control of 18s ribosomal RNA Thermo Fisher Scientific to quantify messenger RNA (mRNA) for AOX1. We used a SYBR (Thermo Fisher Scientific) green master mix to quantify mRNA for GPER1 (forward primer 5'-CGTCCTGTG CACCTTCATGT-3' backward primer 5'-AGCTCATCCAGGTGAGGAAGAA-3')

FIGURE 4
Lipid peroxidation is increased in late-term and stillbirth placentas

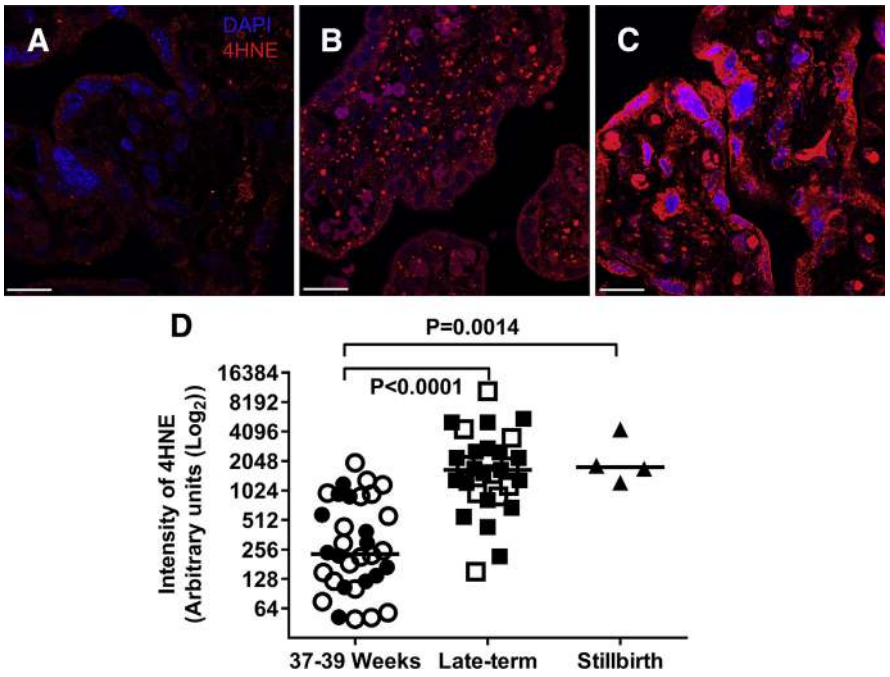

4-Hydroxynonenal (4HNE) (red) immunostaining in **A**, 37- to 39-week, **B**, late-term, and **C**, stillbirth placentas. 4′,6-Diamidino-2-phenylindole (DAPI) (blue) staining identifies nuclei. **D**, Intensity of 4HNE is significantly increased in late-term ($P < .0001$, Mann-Whitney test) and stillbirth ($P = .0014$, Mann-Whitney test) placentas. **D**, Open and filled circles represent 37- to 39-week cesarean nonlaboring (n = 20) and vaginal delivery laboring (n = 14) placentas, respectively; open and filled squares represent late-term laboring cesarean (n = 10) and vaginal delivery (n = 18) placentas, respectively; and filled triangles represent third-trimester laboring vaginal delivery unexplained stillbirth placentas (n = 4). **D**, Each point represents mean intensity per unit area for 6 images taken for each individual placenta. Images were photographed at ×100 magnification; scale bar = 20 μm.

Maiti et al. Fetal death and placental aging. Am J Obstet Gynecol 2017.

(Invitrogen, Waltham, MA) with respect to beta-actin as an internal control using a 7500 PCR system (Applied Biosystems, Foster City, CA).

Statistical analysis

Sample numbers are shown in the legends to individual figures. The data in Figures 2, 4 to 6, and 8 were analyzed using the Mann-Whitney test (2-way) and results are presented as scatter plots showing the median. The data in Figure 7 and Supplementary Figures 2 and 3 were analyzed using the Wilcoxon matched-pairs signed rank test and results are presented as mean showing SEM. All the *P* values were calculated using GraphPad Prism software (Version 7; Graph Pad Software Inc, San Diego, CA). A *P* value of ≤.05 was considered statistically significant.

Results

Subject characteristics

Demographic and clinical characteristics of the study participants are reported in the Table.

Relationship between stillbirth risk and length of gestation

To illustrate the relationship between stillbirth risk and length of gestation we created a Kaplan-Meier plot of the data on human gestational length in a population with relatively low levels of medical intervention from Omigbodun and Adewuyi[10] and combined it with the data on risk of stillbirth per 1000 continuing pregnancies from Sutan et al[2] (Figure 1). The data illustrate that stillbirth is consistent with an aging etiology as defined by Johnson et al.[3]

DNA/RNA oxidation

We sought evidence of placental DNA/RNA oxidation as measured by 8OHdG, as a marker of DNA/RNA oxidation that was previously observed in aging tissues[11] such as the brain in Alzheimer disease.[12] IHC was performed for 8OHdG and the average intensity of 8OHdG staining in nuclei/frame demonstrated a significant increase in DNA/RNA oxidation in late-term and stillbirth-associated placentas (Figure 2).

Movement and clustering of lysosomes in late-term and stillbirth placentas

Misfolded proteins and damaged mitochondria are normally recycled in autophagosomes in a process that involves autophagosome fusion with proteolytic enzyme-containing lysosomes. Accumulation of abnormal protein is thought to play a role in aging, particularly in the brain, for instance the accumulation of tau and amyloid protein in Alzheimer disease[13,14] and mutant huntingtin in Huntington disease.[15] In Huntington disease, the distribution of the lysosomes within neurones is altered with increased perinuclear accumulation of lysosomes.[16] We used a lysosomal marker, LAMP2, to analyze the distribution of lysosomes in the placenta by IHC. IHC showed lysosomes positioned on the apical surface of early-term placental syncytiotrophoblast (Figure 3, A, D, and E), whereas lysosomes relocated to the perinuclear and the basal surface in late-term and stillbirth placentas (Figure 3, B, C, F, and G).

Lipid oxidation in placental tissue

The increase in DNA oxidation that we demonstrated suggested free radical damage that might also lead to lipid peroxidation. Lipid peroxidation

FIGURE 5
Larger autophagosomes occur in late-term and stillbirth placentas

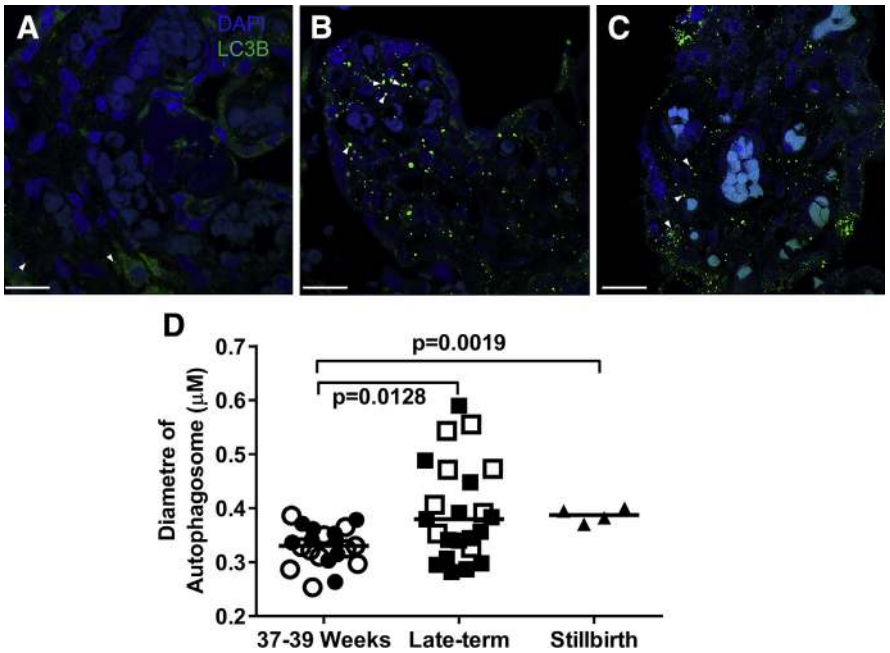

Immunofluorescence staining of LC3B (green) in **A**, 37- to 39-week, **B**, late-term, and **C**, unexplained stillbirth placentas. 4′,6-Diamidino-2-phenylindole (DAPI) (blue) staining indicates nuclei. Autophagosome size was quantified using NIS element (Nikon) software and diameter was measured at arbitrary intensity range of 1000-3000, diameter range 0.2-1 μm, and circularity range 0.5-1. **D**, Analysis showed that late-term and stillbirth placentas have significantly larger ($P = .012$ and $P = .0019$, respectively, Mann-Whitney test) autophagosomes than 37- to 39-week placentas. **D**, Open and filled circles represent 37- to 39-week cesarean nonlaboring (n = 11) and vaginal delivery laboring (n = 10) placentas, respectively; open and filled squares represent late-term laboring cesarean (n = 8) and laboring vaginal delivery (n = 15) placentas, respectively; and filled triangles represent unexplained stillbirth placentas (n = 4). Each point in graph represents average diameter of LC3B particles in 6 images taken for each placenta. Original magnification, ×100; scale bar = 20 μm. Arrowheads indicate autophagosomes (LC3B positive particles).

Maiti et al. Fetal death and placental aging. Am J Obstet Gynecol 2017.

has been observed to increase in Alzheimer disease as measured by the formation of 4HNE.[17] We therefore performed IHC for 4HNE in late-term, stillbirth, and 37- to 39-week placental tissue. This revealed a marked, statistically significant increase in 4HNE staining in late-term syncytiotrophoblast that we also observed in placentas associated with stillbirth shown in Figure 4.

Larger autophagosomes containing 4HNE occur in late-term and stillbirth-associated placentas

Inhibition of autophagosome function with failure of fusion with lysosomes leads to an increase in autophagosome size.[18,19] This process leads to inhibition of overall autophagic function that is seen in Alzheimer disease,[18] Danon disease,[19] and neurodegeneration.[20] We detected autophagosomes using IHC with an antibody against LC3B. We observed a significant increase in the size of autophagosomes (Figure 5, D) in both late-term (Figure 5, B) and stillbirth-associated (Figure 5, C) placentas compared to 37- to 39-week placentas (Figure 5, A). Dual-labeled fluorescence immunostaining showed that the larger autophagosomes of late-term and stillbirth placentas contained 4HNE, a product of lipid peroxidation (Supplementary Figure 1).

Role of AOX1 in placental oxidative damage

AOX1 is a molybdoflavoenzyme, which oxidizes a range of aldehydes including 4HNE into corresponding acids and peroxides.[21] We provide evidence that AOX1 is involved in the generation of the increased 4HNE observed in late-term and stillbirth-associated placentas using colocalization. Dual-labeled fluorescence IHC showed that AOX1 colocalizes to 4HNE-positive particles in late-term (Figure 6, A to C) and stillbirth (Figure 6, D to F) placentas. Additionally, real-time quantitative PCR showed that late-term and stillbirth placentas expressed significantly higher mRNA for AOX1 than 37- to 39-week placentas (Figure 6, G). These data support the concept that AOX1 plays a role in the oxidative damage that occurs in the late-term and stillbirth-associated placentas.

Pharmacological inhibition of AOX1 using placental explant culture

Our data provide clear evidence for increased lipid oxidation, disordered lysosome-autophagosome interactions, and increased AOX1 expression in the late-term and stillbirth placental syncytiotrophoblast. To determine if these events were causally linked we developed a placental explant culture system using term placental tissue cultured in serum-free (growth factor−deficient) medium. IHC showed that serum deprivation significantly increased production of 4HNE at 24 hours after incubation (Figure 7, A to C, F, and G). We also found a significant increase in the size of autophagosomes (Supplementary Figure 2) and a change in lysosomal distribution to a perinuclear location >24-hour incubation in serum-free medium (Supplementary Figure 3). We sought to determine cause-and-effect relationships between the development of lipid oxidation observed when placental explants were cultured in the

FIGURE 6
Colocalization of AOX1 and 4HNE and increased AOX1-mRNA in stillbirth

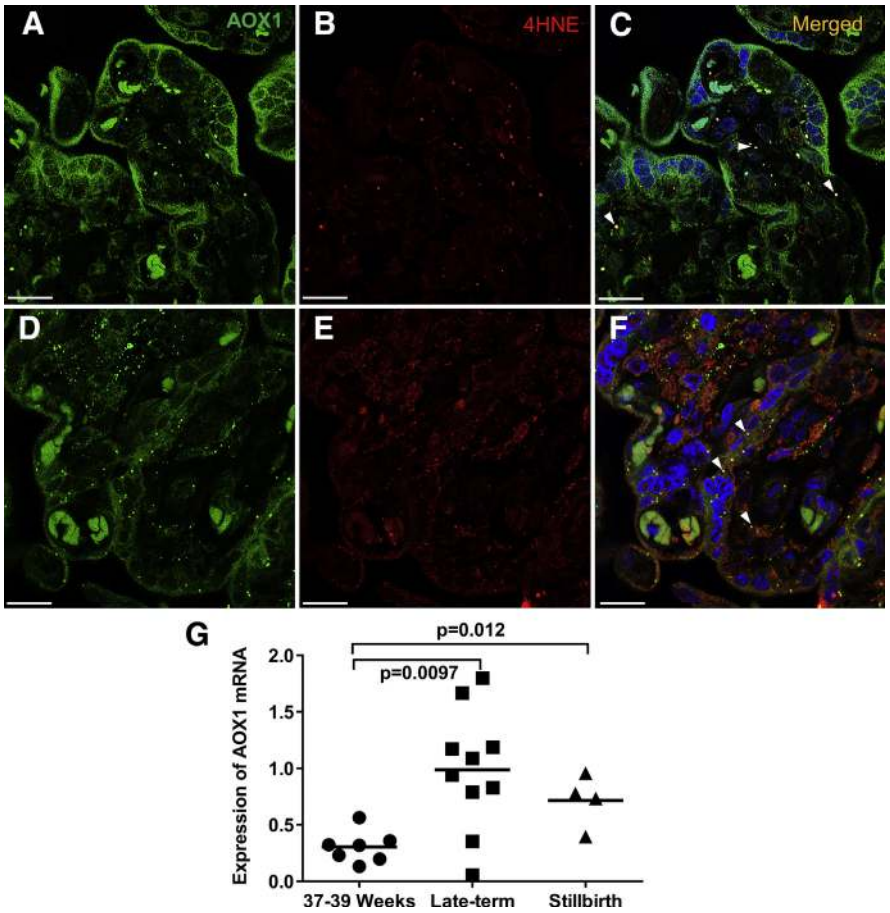

Representative dual-labeled fluorescence immunostaining in **A** to **C**, late-term and **D** to **F**, stillbirth placentas showed that AOX1-positive particles (green) are colocalized with 4HNE (red). **C** and **F**, Orange dots (arrowheads) indicate colocalization. Nuclei are stained with 4′,6-diamidino-2-phenylindole (blue). **G**, Real-time polymerase chain reaction showed that expression of AOX1 mRNA is increased in late-term ($P = .0097$) and stillbirth ($P = .012$) placentas compared to early-term placentas. Original magnification ×100; scale bar = 20 μm.

Maiti et al. Fetal death and placental aging. Am J Obstet Gynecol 2017.

absence of serum, and AOX1. To achieve this we used a potent AOX1 inhibitor, raloxifene[22] and a GPER1 agonist, G1. We used the GPER1 agonist G1 as we had detected GPER1 expression on the apical surface of syncytiotrophoblast (Figure 8, A and B) and the GPER1 agonist has been shown to inhibit production of 4HNE in the kidney.[23] Both raloxifene and G1 inhibited the production of 4HNE in the serum-starved placental explants >24 hours of treatment (Figure 7, D to G). G1 also prevented the changes in lysosomal distribution within the syncytiotrophoblast (Supplementary Figure 3).

Presence of the cell surface estrogen receptor GPER1 on the apical surface of the syncytiotrophoblast

As the GPER1 agonist had evident effects in placental explant cultures we undertook characterization of GPER1 expression in placental tissue. The expression of GPER1 in a section of placenta roll (described in the "Materials and Methods" section) detected by fluorescent IHC showed that GPER1 is expressed in placental villi (Figure 8, A), which, at higher magnification (×100), was localized to the apical surface of placental villi (Figure 8, B). Real-time PCR for GPER1 showed that placental villi have significantly higher expression of GPER1 than amnion, chorion, or decidua (Figure 8, C). Western blot for GPER1 also confirmed higher protein levels of GPER1 in placental villous tissue than amnion, chorion, or decidua (Figure 8, D). The demonstration of GPER1 localization on the apical surface of the syncytiotrophoblast indicates the plausibility of estrogen inhibition of AOX1 activity in the placenta.

Comment

Our data indicate that between 37-39 and 41 weeks of gestation dramatic changes occur in the biochemistry and physiology of the placenta. In particular there is increased oxidative damage to DNA/RNA and lipid, a change in position of lysosomes that accumulate at the perinuclear and basal surface of the syncytiotrophoblast, the formation of larger autophagosomes associated with oxidized lipid, and increased expression of the enzyme AOX1. The same changes are observed in placentas associated with stillbirth. Some of our results are semiquantitative as this is the nature of Western analysis; nevertheless, the robustness of our results is supported by the use of multiple end points for aging, and the biological plausibility of the reported links. Further supporting our hypothesis, similar changes in oxidation of lipid, localization of lysosomes, and size of autophagosomes occurred in placental explants deprived of growth factors, and these changes were blocked by inhibition of AOX1.

Stillbirth occurs in approximately 1 in 200 pregnancies in developed countries.[1] The *Lancet*[1] and the *BMJ*[24]

FIGURE 7
Pharmacologic inhibition of 4-hydroxynonenal (4HNE) production

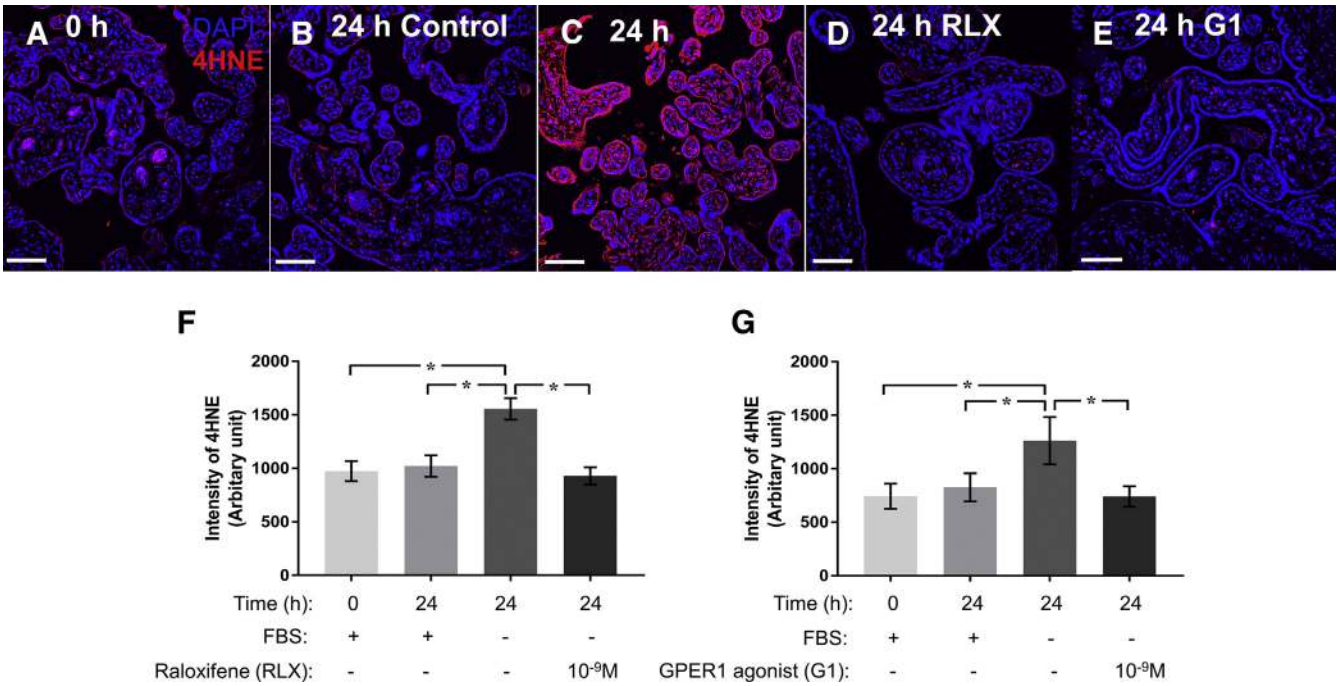

Fluorescence immunostaining with antibody against 4HNE (red) in **A**, serum-starved placental explant at time 0 (just before starvation); **B**, 24 hours after culturing in medium containing fetal bovine serum (FBS) (control treatment); **C**, 24 hours after starvation (culturing in medium without FBS); **D**, 24 hours after treatment with aldehyde oxidase 1 inhibitor, raloxifene (RLX); and **E**, 24 hours after treatment with membrane estrogen receptor G-protein-coupled estrogen receptor 1 agonist, G1. Intensity calculation showed that production of 4HNE (induced by serum starvation) is significantly reduced after treating placental explants with **F**, RLX and **G**, G1. Data are mean ± SEM, $^*P < .05$ (N = 6). Original magnification, ×20; scale bar = 100 μm. 4′,6-Diamidino-2-phenylindole (DAPI) (blue) staining indicates nuclei.

Maiti et al. Fetal death and placental aging. Am J Obstet Gynecol 2017.

recently highlighted gaps in our knowledge of this condition. Stillbirth frequently occurs in the setting of fetal growth restriction and in this setting telomere shortening and oxidative damage have been observed in associated placentas.[25] The risk of stillbirth per 1000 continuing pregnancies rises dramatically >38 weeks of gestation. We have suggested[4] that stillbirths in late gestation are a consequence of placental aging. More than 90% of pregnancies have delivered by the end of the 40th week of gestation,[10] consequently changes that occur in the placenta in pregnancies that have gone past the usual term have little effect on population-level infant survival, since most have already delivered. Such late-gestation changes may exist in a kind of Medawar[26] shadow that allows deleterious genes to persist in the population if their damaging effects occur after reproduction, especially if the same genes exert positive actions earlier in pregnancy. This Medawar[26] shadow effect has been proposed to explain the high prevalence of Huntington disease associated with increased fertility in early life but disastrous neurological deterioration after reproduction has occurred.[27] Our immunofluorescence data show high levels of 8OHdG and 4HNE in late-term and stillbirth placentas supporting this postulated pathway to placental aging. Increases in oxidative damages to DNA and lipid have also been reported in Alzheimer disease.[17,28]

We have also seen marked accumulation of particles positive for the lysosomal marker LAMP2 in the perinuclear and basal side of the syncytiotrophoblast of late-term placentas and placentas associated with stillbirth. This phenomenon closely resembles lysosomal positioning that occurs in cells under nutritional stress.[29] Autophagy is an important cellular recycling process that involves fusion of acidic lysosomes with the autophagosomes. Our data show that stillbirth and late-term placentas contain larger autophagosomes than 37- to 39-week placentas indicating inhibition of the autophagic process in these placentas. Our data further indicate that the autophagosomes are coated with oxidized lipid in the form of 4HNE, which may play a role in the failure of lysosomal-autophagosome fusion. Such disturbances in the function of

FIGURE 8
Expression of GPER1 in placenta and myometrium

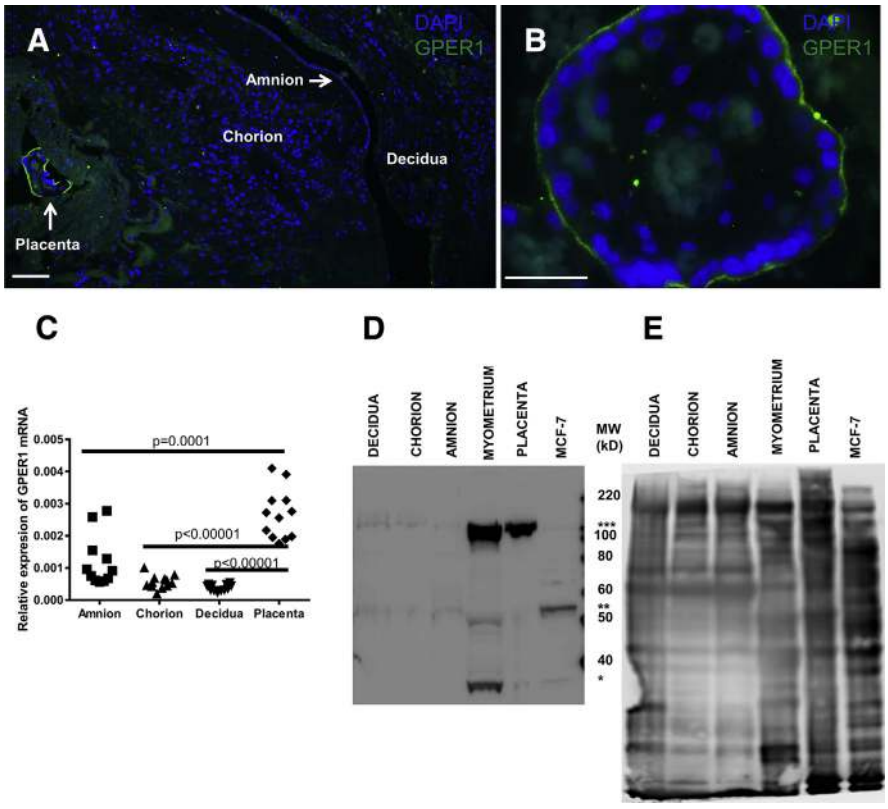

Fluorescence IHC showed that GPER1 (green) is localized predominantly in placenta in section of term placental roll photographed at **A**, ×10 magnification. **B**, GPER1 (green) was shown to localize in apical layer of syncytiotrophoblast of placental villi when photographed at ×100 magnification. **A** and **B**, Scale bar = 100 and 20 μm, respectively. **C**, Real-time quantitative PCR data showed that messenger RNA (mRNA) for GPER1 is expressed in higher amounts in term placenta, whereas amnion, chorion, and decidua show very low expression of GPER1. Expression of mRNA for GPER1 follows order: decidua<chorion<amnion<placenta. **D**, Western blot of protein extract from breast cancer cell line Michigan Cancer Foundation-7 (MCF-7), term placenta, myometrium, amnion, chorion, and decidua. **D**, Placenta, myometrium, and MCF-7 cell lines expressed higher amounts of GPER1 than amnion, chorion, or decidua. Western-blotting data showed that all tissues expressed glycosylated GPER1 (** or ***) and nonglycosylated nascent GPER1 (*). **E**, SYPRO Ruby stain (Thermo Fisher Scientific) of same polyvinylidene fluoride membrane is used as internal loading control.

DAPI, 4′,6-diamidino-2-phenylindole; *MW*, molecular weight.

Maiti et al. Fetal death and placental aging. Am J Obstet Gynecol 2017.

autophagosomes may lead to the accumulation of abnormal protein and deterioration in the function of the syncytiotrophoblast.

Stillbirth is not restricted to the late-term setting and is known to be associated with cigarette smoking and growth restriction. It seems likely that smoking accelerates aging-related pathways. Evidence for this is the finding that telomere length is reduced in the fetuses of women who actively smoke during pregnancy,[30] and similar changes are to be expected in the placentas of smokers. Down syndrome is associated with advanced aging or progeria[31,32] and with increased rates of stillbirth,[33,34] raising the possibility that accelerated placental aging may play a part in stillbirth related to Down and some other congenital anomalies. Similarly placental abruption is associated with growth restriction, maternal smoking, and stillbirth, and placental aging may play a part in this condition.[35,36]

We used cultured term placental explants to interrogate the pathways leading to the lipid oxidation and disturbed autophagosome function. We measured production of 4HNE and the diameter of autophagosomes following serum depletion. We observed a significant increase in 4HNE and a significant increase in autophagosome size suggesting inhibition of autophagy by oxidative damage as we previously observed in the stillbirth and late-term placentas. Raloxifene, a potent inhibitor of AOX1, has been shown to reduce oxidative damage in endothelial cells.[37] We demonstrated that the AOX1 inhibitor raloxifene is also able to block oxidative damage to the lipid in placental explants. The role of AOX1 was confirmed using the GPER1 agonist G1 that has been shown to block AOX1 activation and reduce 4HNE in renal tissue.[23] G1 also blocked changes in lysosomal positioning within the explants. We report the novel finding of the presence of the cell surface estrogen receptor GPER1 on the syncytiotrophoblast apical membrane, suggesting that this receptor may play a role in modulating oxidative damage within the placenta. It has been shown that urine from pregnant women carrying a fetus with postmaturity syndrome has lower estrogen:creatinine ratios than that from women carrying normal fetuses.[38] These data support the possibility that low estrogen concentrations may lead to loss of the cell surface estrogen receptor (GPER1) mediated inhibition of AOX1 and consequently placental oxidative damage and impaired function.

The changes in the late-term placenta occur as the fetus continues to grow and to require additional supplies of nutrients. Postmaturity

TABLE
Demographic and clinical characteristics of study subjects

CC Characteristic	37-39 wk	Late-term	Stillbirth			
Cases, n	34	28	4			
Gestational ages, wk	38.57 ± 0.15	41.46 ± 0.06	32	32.57	39	40.14
Fetal growth restriction, n	0	0	No	Yes	No	Yes
Maternal age, y	31.03 ± 0.88	28.81 ± 1.15	30.21 ± 2.68			
Vaginal birth	41.20%	64.30%	100.00%			
BMI, kg/m^2, at second trimester or at birth	29.10 ± 1.50	28.52 ± 1.10	27.40 ± 2.40			
Ethnicity						
Caucasian	82.35%	96.42%	75.00%			
Smoker	17.64%	17.85%	0.00%			

Data are presented as (mean ± SEM) or percentage unless otherwise specified.

BMI, body mass index.

Maiti et al. Fetal death and placental aging. Am J Obstet Gynecol 2017.

syndrome is a condition seen in postdates infants who show evidence of late gestation failure of nutrition.[39] Normal human infants born at term have 12-14% body fat whereas postmaturity syndrome is associated with the birth of a baby with severe wrinkling of the skin due to loss of subcutaneous fat. Postmaturity syndrome is rarely seen in modern obstetric practice where delivery is usually effected <42 weeks of gestation using induction of labor or cesarean delivery if labor has not occurred spontaneously. While none of the infants born to mothers in our study exhibited postmaturity syndrome, our data suggest that the physiological function of the placenta >41 completed weeks is showing evidence of decline that has many features in common with aging in other tissues. The known exponential increase in unexplained intrauterine death that occurs >38 weeks of gestation may therefore be a consequence of aging of the placenta and decreasing ability to adequately supply the increasing needs of the growing fetus. This knowledge may impact on obstetric practice to ensure infants are born before the placenta ages to the point of critical failure.[40] However, it is notable that not all placentas in our late-term cohort exhibited evidence of aging and it is known that infants born later in gestation have lower rates of special school needs, with those born at 41 weeks having the lowest rates.[41] The conflicting pressures of late gestation increases in stillbirth and falling rates of intellectual disability make obstetric care at this time very challenging; diagnostics that can predict pregnancies at increased risk of stillbirth would be useful and some progress in their development has been made.[42] Our data also indicate that the placenta may provide a tractable model of aging in a human tissue that uniquely ages in a 9-month period of time. The results suggest that the rate of aging of the placenta varies in different pregnancies and raises the possibility that the rate of aging of the placenta may parallel the rate of aging of the associated fetus carrying the same genome. Our work identifies potential therapeutic targets such as AOX1 that may arrest the oxidative damage to placentas in pregnancies identified at high risk of stillbirth when extreme prematurity precludes delivery. Finally, our data raise the possibility that markers of placental oxidative damage and AOX1 mRNA may be released into maternal blood where they may have diagnostic value in predicting the fetus at risk for stillbirth. ■

Acknowledgment

The authors would like to thank Mrs Anne Wright (midwife); all nurses and doctors of John Hunter Hospital, Australia, for helping in collection of placental tissues; and especially the women who donated their tissues. The authors acknowledge the contribution of Dr Carolyn Mitchell for providing complementary DNA for amnion, chorion, and decidua.

References

1. Flenady V, Middleton P, Smith GC, et al. Stillbirths: the way forward in high-income countries. Lancet 2011;377:1703-17.
2. Sutan R, Campbell D, Prescott G, Smith W. The risk factors for unexplained antepartum stillbirths in Scotland, 1994 to 2003. J Perinatol 2010;30:311-8.
3. Johnson FB, Sinclair DA, Guarente L. Molecular biology of aging. Cell 1999;96:291-302.
4. Smith R, Maiti K, Aitken R. Unexplained antepartum stillbirth: a consequence of placental aging? Placenta 2013;34:310-3.
5. Amir H, Weintraub A, Aricha-Tamir B, Apel-Sarid L, Holcberg G, Sheiner E. A piece in the puzzle of intrauterine fetal death: pathological findings in placentas from term and preterm intrauterine fetal death pregnancies. J Matern Fetal Neonatal Med 2009;22:759-64.
6. Labarrere CA, Dicarlo HL, Bammerlin E, et al. Failure of physiologic transformation of spiral arteries, endothelial and trophoblast cell activation, and acute atherosis in the basal plate of the placenta. Am J Obstet Gynecol 2017;216:287.e1-16.
7. Ferrari F, Facchinetti F, Saade G, Menon R. Placental telomere shortening in stillbirth: a sign

of premature senescence? J Matern Fetal Neonatal Med 2016;29:1283-8.
8. Biron-Shental T, Sukenik-Halevy R, Sharon Y, et al. Short telomeres may play a role in placental dysfunction in preeclampsia and intrauterine growth restriction. Am J Obstet Gynecol 2010;202:381.e1-7.
9. Maiti K, Paul J, Read M, et al. G-1-activated membrane estrogen receptors mediate increased contractility of the human myometrium. Endocrinology 2011;152:2448-55.
10. Omigbodun AO, Adewuyi A. Duration of human singleton pregnancies in Ibadan, Nigeria. J Natl Med Assoc 1997;89:617.
11. Hirano T, Yamaguchi R, Asami S, Iwamoto N, Kasai H. 8-Hydroxyguanine levels in nuclear DNA and its repair activity in rat organs associated with age. J Gerontol A Biol Sci Med Sci 1996;51:B303-7.
12. Lovell MA, Markesbery WR. Oxidative DNA damage in mild cognitive impairment and late-stage Alzheimer's disease. Nucleic Acids Res 2007;35:7497-504.
13. Hardy J, Selkoe DJ. The amyloid hypothesis of Alzheimer's disease: progress and problems on the road to therapeutics. Science 2002;297:353-6.
14. Goedert M, Spillantini M, Jakes R, Rutherford D, Crowther R. Multiple isoforms of human microtubule-associated protein tau: sequences and localization in neurofibrillary tangles of Alzheimer's disease. Neuron 1989;3:519-26.
15. Carter RJ, Lione LA, Humby T, et al. Characterization of progressive motor deficits in mice transgenic for the human Huntington's disease mutation. J Neurosci 1999;19:3248-57.
16. Erie C, Sacino M, Houle L, Lu ML, Wei J. Altered lysosomal positioning affects lysosomal functions in a cellular model of Huntington's disease. Eur J Neurosci 2015;42:1941-51.
17. Markesbery W, Lovell M. Four-hydroxynonenal, a product of lipid peroxidation, is increased in the brain in Alzheimer's disease. Neurobiol Aging 1998;19:33-6.
18. Boland B, Kumar A, Lee S, et al. Autophagy induction and autophagosome clearance in neurons: relationship to autophagic pathology in Alzheimer's disease. J Neurosci 2008;28:6926-37.
19. Tanaka Y, Guhde G, Suter A, et al. Accumulation of autophagic vacuoles and cardiomyopathy in lamp-2-deficient mice. Nature 2000;406:902-6.
20. Lee J-A, Beigneux A, Ahmad ST, Young SG, Gao F-B. Escrt-iii dysfunction causes autophagosome accumulation and neurodegeneration. Curr Biol 2007;17:1561-7.
21. Garattini E, Terao M. Increasing recognition of the importance of aldehyde oxidase in drug development and discovery. Drug Metab Rev 2011;43:374-86.
22. Obach RS. Potent inhibition of human liver aldehyde oxidase by raloxifene. Drug Metab Dispos 2004;32:89-97.
23. Lindsey SH, Yamaleyeva LM, Brosnihan KB, Gallagher PE, Chappell MC. Estrogen receptor gpr30 reduces oxidative stress and proteinuria in the salt-sensitive female mren2.Lewis rat. Hypertension 2011;58:665-71.
24. Gardosi J, Madurasinghe V, Williams M, Malik A, Francis A. Maternal and fetal risk factors for stillbirth: population based study. BMJ 2013;346:f108.
25. Davy P, Nagata M, Bullard P, Fogelson N, Allsopp R. Fetal growth restriction is associated with accelerated telomere shortening and increased expression of cell senescence markers in the placenta. Placenta 2009;30:539-42.
26. Medawar PB. An unsolved problem of biology. London: University College; 1952.
27. Eskenazi BR, Wilson-Rich NS, Starks PT. A Darwinian approach to Huntington's disease: subtle health benefits of a neurological disorder. Med Hypotheses 2007;69:1183-9.
28. Lovell MA, Gabbita SP, Markesbery WR. Increased DNA oxidation and decreased levels of repair products in Alzheimer's disease ventricular csf. J Neurochem 1999;72:771-6.
29. Korolchuk VI, Saiki S, Lichtenberg M, et al. Lysosomal positioning coordinates cellular nutrient responses. Nat Cell Biol 2011;13:453-60.
30. Salihu HM, Pradhan A, King L, et al. Impact of intrauterine tobacco exposure on fetal telomere length. Am J Obstet Gynecol 2015;212:205.e1-8.
31. Adorno M, Sikandar S, Mitra SS, et al. Usp16 contributes to somatic stem-cell defects in Down's syndrome. Nature 2013;501:380-4.
32. Souroullas GP, Sharpless NE. Stem cells: Down's syndrome link to aging. Nature 2013;501:325-6.
33. Morris JK, Wald NJ, Watt HC. Fetal loss in Down syndrome pregnancies. Prenat Diagn 1999;19:142-5.
34. Frey HA, Odibo AO, Dicke JM, Shanks AL, Macones GA, Cahill AG. Stillbirth risk among fetuses with ultrasound-detected isolated congenital anomalies. Obstet Gynecol 2014;124:91-8.
35. Ananth CV, Williams MA. Placental abruption and placental weight—implications for fetal growth. Acta Obstet Gynecol Scand 2013;92:1143-50.
36. Matsuda Y, Hayashi K, Shiozaki A, Kawamichi Y, Satoh S, Saito S. Comparison of risk factors for placental abruption and placenta previa: case-cohort study. J Obstet Gynaecol Res 2011;37:538-46.
37. Wassmann S, Laufs U, Stamenkovic D, et al. Raloxifene improves endothelial dysfunction in hypertension by reduced oxidative stress and enhanced nitric oxide production. Circulation 2002;105:2083-91.
38. Rayburn WF, Motley ME, Stempel LE, Gendreau RM. Antepartum prediction of the postmature infant. Obstet Gynecol 1982;60:148-53.
39. Moya F, Grannum P, Pinto K, Bracken M, Kadar N, Hobbins JC. Ultrasound assessment of the postmature pregnancy. Obstet Gynecol 1985;65:319-22.
40. Nicholson JM, Kellar LC, Ahmad S, et al. US term stillbirth rates and the 39-week rule: a cause for concern? Am J Obstet Gynecol 2016;214:621.e1-9.
41. Mackay DF, Smith GC, Dobbie R, Pell JP. Gestational age at delivery and special educational need: retrospective cohort study of 407,503 schoolchildren. PLoS Med 2010;7:e1000289.
42. Chaiworapongsa T, Romero R, Korzeniewski SJ, et al. Maternal plasma concentrations of angiogenic/anti-angiogenic factors in the third trimester of pregnancy to identify the patient at risk for stillbirth at or near term and severe late preeclampsia. Am J Obstet Gynecol 2013;208:287.e1-15.

Author and article information

From the Mothers and Babies Research Center, Hunter Medical Research Institute, Newcastle, Australia (Drs Maiti and Smith, and Ms Sultana); Priority Research Center in Reproductive Science, Faculty of Health, University of Newcastle, Newcastle, Australia (Drs Maiti, Aitken, and Smith, and Ms Sultana); Kolling Institute, Royal North Shore Hospital, University of Sydney, Sydney, Australia (Dr Morris); Department of Obstetrics and Gynecology, John Hunter Hospital, Newcastle, Australia (Drs Park and Andrew); and MRC Center for Reproductive Health, University of Edinburgh, Edinburgh, United Kingdom (Dr Riley).

Received May 1, 2017; revised June 6, 2017; accepted June 13, 2017.

This study was funded by John Hunter Hospital Charitable Trust Grant 2013 (G1300740), Stillbirth Foundation Australia Grant 2014 (G1400089), Haggarty Foundation, and National Health and Medical Research Council grant (APP1084782).

K.M. and R.S. hold patents through the University of Newcastle on aldehyde oxidase 1 as a therapeutic target and the use of placental aging-related markers as diagnostics to predict stillbirth.

Corresponding author: Roger Smith, PhD, MBBS. roger.smith@newcastle.edu.au

SUPPLEMENTARY FIGURE S1

Oxidized lipids within autophagosomes of late-term placentas

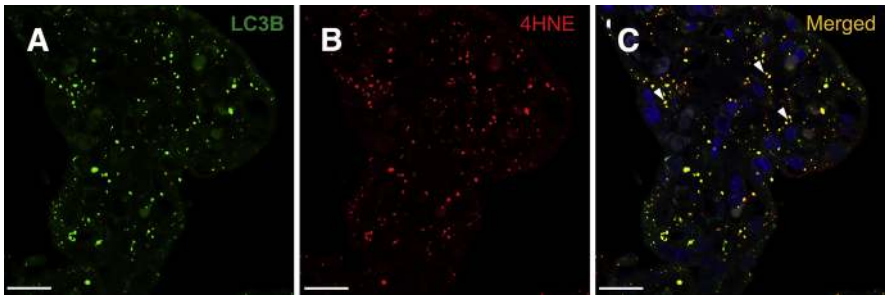

Representative dual-labeled fluorescence immunostaining showed that **A**, LC3B, autophagosome marker (green), is colocalized with **B**, 4-hydroxynonenal (4HNE), marker of lipid peroxidation (red). **C**, Orange dots (arrowheads) indicate colocalization. 4′,6-Diamidino-2-phenylindole (blue) staining indicates nuclei. Original magnifications ×100; scale bar = 20 μm.

Maiti et al. Fetal death and placental aging. Am J Obstet Gynecol 2017.

SUPPLEMENTARY FIGURE S2

Changes in autophagosome size in placental-explants cultured in serum-deprived medium

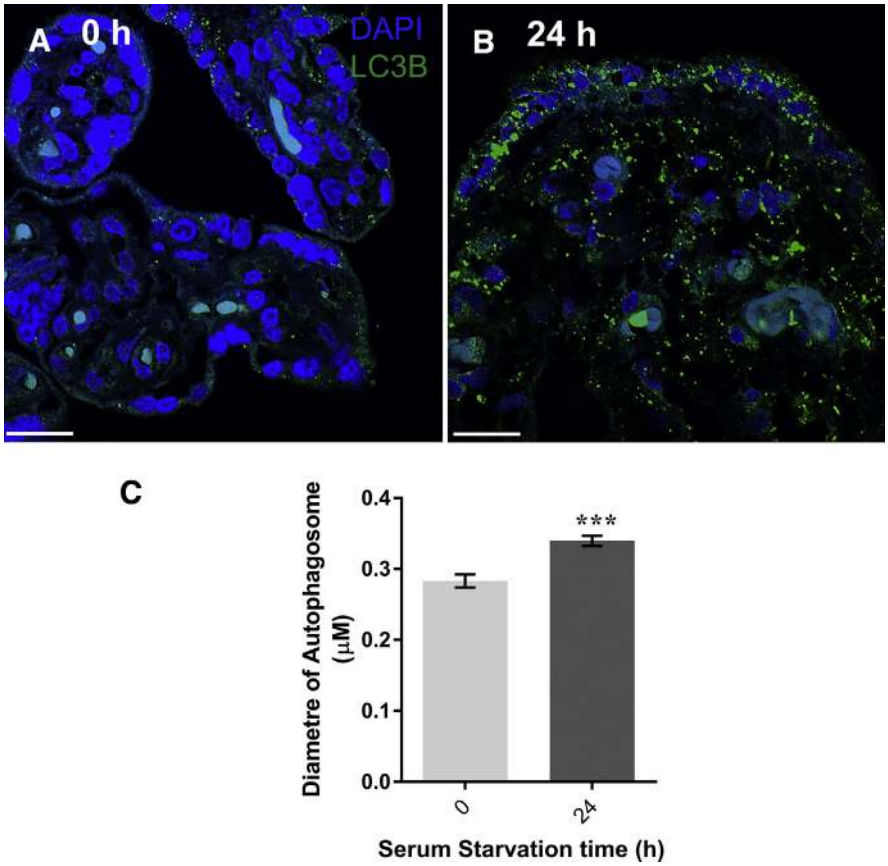

Fluorescence immunostaining with antibody against LC3B (green) in **A**, serum-starved placental explant at time 0 (just before starvation) and **B**, 24 hours after starvation. 4′,6-Diamidino-2-phenylindole (DAPI) (blue) staining indicates nuclei. **C**, Immunohistochemical analysis showed that size of autophagosomes (LC3B-positive particles) increased 24 hours after serum starvation compared to 0 hours. Data presented as mean ± SEM, ***$P = .0002$ (N = 13). Scale bar = 20 μm.

Maiti et al. Fetal death and placental aging. Am J Obstet Gynecol 2017.

SUPPLEMENTARY FIGURE S3
GPER1 regulates lysosomal distribution in placental-explants cultured in serum-deprived medium

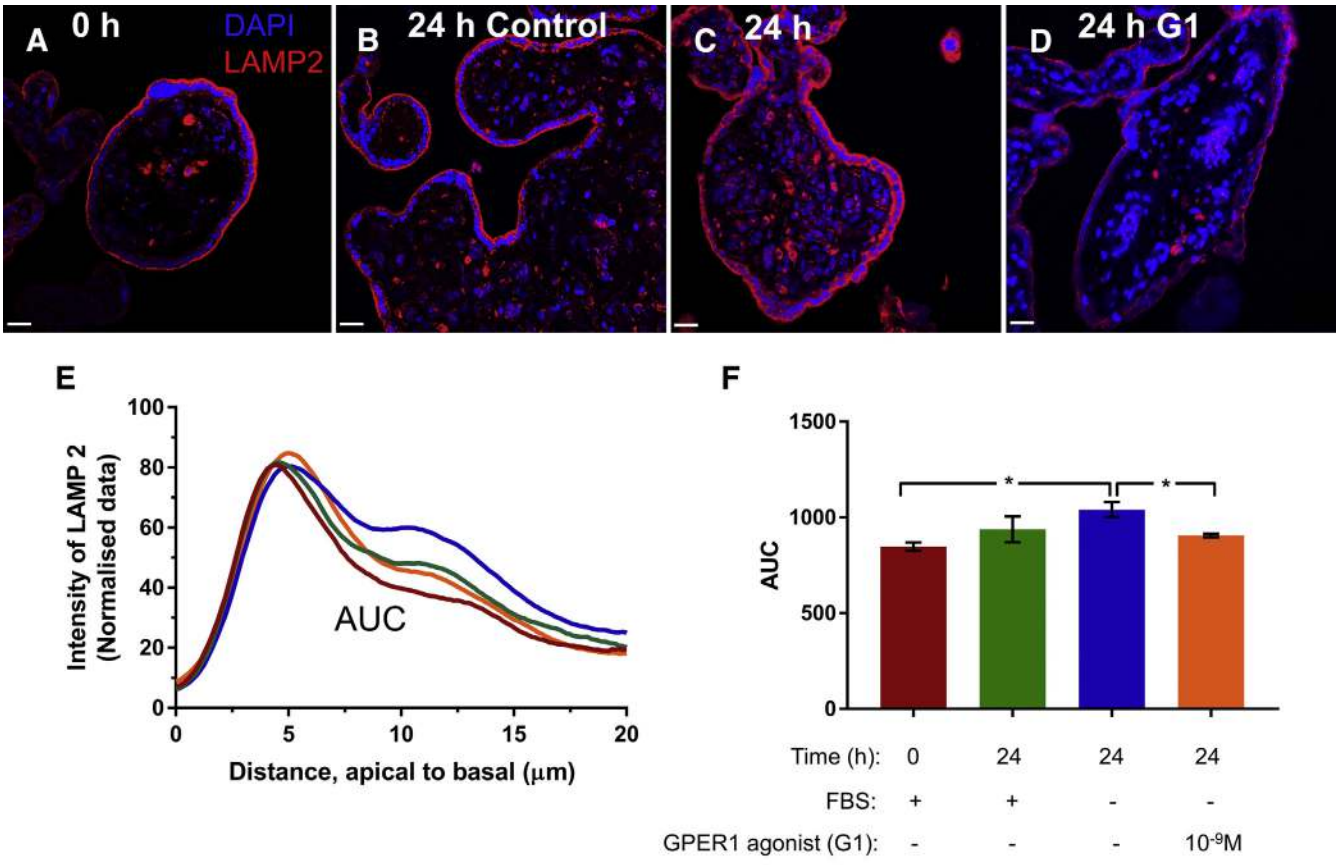

Fluorescence immunostaining with antibody against lysosome-associated membrane protein 2 (LAMP2) (red) in **A**, serum-starved placental explant at time 0 (just before starvation); **B**, 24 hours after culturing in medium containing fetal bovine serum (FBS); **C**, 24 hours after starvation (culturing in medium without) FBS; and **D**, 24 hours after treatment with GPER agonist, G1. 4′,6-Diamidino-2-phenylindole (DAPI) (blue) staining indicates nuclei. **E**, Intensity calculation across syncytiotrophoblast showed that distribution of LAMP2 at 24 hours after starvation shifts to perinuclear and basal surface compared to control treatment (N = 7). **E**, Each colored line represents mean intensity of LAMP2 across syncytiotrophoblast at 5 random sites per image for 6 separate images per experiment. **E**, Each colored bar indicates mean of area under curve (AUC) of corresponding colored line and statistical differences were calculated. Original magnifications, ×40; scale bar = 20 μm; error bar, SEM; *$P < .05$ (N = 7).

Maiti et al. Fetal death and placental aging. Am J Obstet Gynecol 2017.